

## Fully Developed Traveling-Wave Convection in Binary Fluid Mixtures

W. Barten,<sup>(1)</sup> M. Lücke,<sup>(1)</sup> W. Hort,<sup>(1)</sup> and M. Kamps<sup>(2)</sup>

<sup>(1)</sup>*Institut für Theoretische Physik, Universität des Saarlandes, D-6600 Saarbrücken, Germany*

<sup>(2)</sup>*Institut für Festkörperforschung der Kernforschungsanlage Jülich, D-5170 Jülich, Germany*

(Received 2 November 1988)

Structural and dynamical properties of nonlinear traveling-wave states in binary fluid layers heated from below are determined by numerical integration of the proper hydrodynamic field equations with experimental horizontal boundary conditions. The fluid separates into traveling rolls of alternating high and low concentration. Phase differences drive lateral currents and Reynolds stresses lateral mean flow.

PACS numbers: 47.25.Qv, 47.20.-k, 47.35.+i

Horizontal layers of binary fluid mixtures, e.g., ethanol and water, heated from below show various structure-forming, convective bifurcations out of the quiescent conductive state.<sup>1-6</sup> In particular, there is a backwards Hopf bifurcation with a hysteretic transition to a convective traveling-wave (TW) state. Therein a *pattern* reminiscent of simple straight convective rolls propagates with uniform velocity. We have elucidated the structure and dynamics of such states: For not too small Soret-induced concentration gradients the fluid separates into an alternating sequence of roll-like domains with homogeneously high and low alcohol concentration and a thin transition boundary layer meandering around the rolls; and this structure propagates as a whole. The waves of temperature  $T$ , alcohol concentration  $C$ , total mass density  $\rho$ , velocity  $\mathbf{u}$ , and pressure  $p$  associated with this TW state are neither planar nor harmonic. Also, there are phase differences between the waves which drive stationary lateral convective currents that are counterflowing in the upper and lower half of the layer. Furthermore, and in addition, the Reynolds stresses of the TW create a global stationary lateral mean flow that is peaked at midheight.

Our results follow from numerically solving the full nonlinear, time-dependent hydrodynamic equations for the fields  $T, C, p$ , and  $\mathbf{u} = (u, 0, w)$  with vertical component  $w$  and lateral component  $u$  in an  $x$ - $z$  section of the layer with rigid, isothermal, impermeable horizontal boundaries at  $z = 0$  and  $d$ . Here  $d$  is the layer thickness. Laterally we impose at  $x = 0$  and  $2d$  periodic boundary conditions—experimental wavelengths of convective roll patterns are  $\lambda \approx 2d$ . We used a MAC code<sup>7</sup> with  $42 \times 22$  grid points. From runs with poorer and better resolution we can infer that all properties of the fields shown here are reproduced correctly. We estimate relevant errors of  $\mathbf{u}, T, C \lesssim 5\%$  ( $10\%$ ). The Prandtl number  $\sigma = \nu/\kappa = 10$ , the Lewis number  $L = D/\kappa = 0.01$ , and separation ratio  $\psi = -(\beta/\alpha T_0)k_T = -0.6$  were for ethanol-water mixtures<sup>8</sup> of mean alcohol concentration  $C_0 \approx 0.08$  and mean temperature  $T_0 = 282$  K. Here  $\nu$  is the kinematic viscosity,  $\kappa$  is the thermal diffusivity,  $D$  is the diffusion coefficient,  $\alpha = -(1/\rho)\partial\rho/\partial T$  and  $\beta = -(1/\rho)\partial\rho/\partial C$  are

thermal and solutal expansion coefficients, and  $k_T$  is the thermodiffusion ratio.<sup>9</sup> We parametrize the vertically imposed temperature difference  $\Delta T$  by  $r = R/R_c^0$ , the Rayleigh number  $R = \alpha g d^3 \Delta T / \kappa \nu$  reduced by the critical one  $R_c^0 = 1708$  for the onset of convection in pure water ( $\psi = 0$ ). Here  $g$  is the gravitational constant. We shall measure lengths in units of  $d$  and time in units of the thermal diffusion time  $d^2/\kappa$ . Temperatures will be reduced by  $\Delta T$  and concentration by  $\Delta T \alpha/\beta$ .

In the quiescent, laterally homogeneous conductive state,  $F_{\text{cond}} = F_0 + s(z - \frac{1}{2})$ , the fields  $F = T, C, \rho$  have vertical gradients  $s = -1, -\psi, \rho_0 \alpha \Delta T (1 + \psi)$ , respectively. The imposed  $\Delta T$  generates via the Soret effect<sup>1</sup> an adverse concentration gradient when  $\psi < 0$ . The density variation arises from thermal and solutal expansion around the mean density  $\rho_0$ . Since the temperature-induced unstable density stratification is reduced at  $\psi < 0$  by the concentration gradient, onset of convection in the mixture occurs at a threshold Rayleigh number  $r > 1$ . For presentation purposes we decompose the fields into conductive parts and contributions caused by convection,

$$\begin{aligned} T - T_{\text{cond}} &= \theta, & C - C_{\text{cond}} &= c, \\ (\rho - \rho_{\text{cond}})/\rho_0 &= \tilde{\rho} = -\alpha \Delta T (\theta + c). \end{aligned} \quad (1)$$

For our parameters an unstable TW solution (with wave number  $k = \pi$  and Hopf frequency  $\omega_H = 23.4$ ) bifurcates subcritically at  $r_{\text{osc}} = 2.41$  out of the conductive state<sup>10</sup> (cf. Fig. 1). Increasing  $r$  beyond  $r_{\text{osc}}$  the system

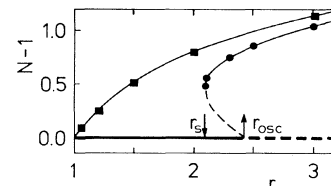


FIG. 1. Nusselt number for TW convective (dots) in mixtures ( $L = 0.01$ ,  $\psi = -0.6$ ) and for stationary rolls in pure fluid (squares) each with  $\sigma = 10$ .  $N = 1$  is the conductive state.

undergoes a transition to the stable upper TW solution branch having a saddle at  $r_s \approx 2.09$ . (For less negative  $\psi$  this TW solution branch ends with zero frequency in a stationary state in the  $r$  range of Fig. 1. The end point moves with increasing  $\psi$  closer to the saddle and falls below  $r_{osc}$ .) Here we present as a representative example the TW at  $r = 2.5 \approx 1.04 r_{osc}$ . After transients have died out all fields have the form of waves traveling, e.g., to the right:  $F = F(x - \omega t/k, z)$ . Their velocity is about  $\frac{1}{3}$  of the linear TW at onset. The Nusselt number is stationary and rather large,  $N = 1.87$ , so that convection is well developed. In Fig. 2 we show isolines of  $T$  and  $C$ . The velocity field looks like that of stationary rolls in pure water. However, the differences are subtle and important (cf. later).

The temperature distribution roughly reflects the velocity field: Warm upflow (cold downflow) bends the horizontal isotherms of the conductive state upwards (downwards). The isotherms are not sinusoidal and their extrema do not coincide with upflow and downflow maxima. In fact, the temperature wave lags behind the wave of the vertical velocity by a phase difference  $\varphi_w - \varphi_\theta \approx 0.38$  that drives a large-scale convective lateral heat current to be discussed later on. The lag agrees well with the prediction  $\arctan[\omega/(k^2 + \pi^2)]$  of a Galerkin model.<sup>5</sup> To display the phase relations of the different waves we show by full lines the crest positions of the first lateral harmonics which dominate. The wave in  $C$  is ahead of the wave in  $w$  and the phase difference  $\varphi_w - \varphi_c$  drives a lateral convective concentration current.

All waves are nonplanar. The  $z$  variation of the lines of constant phases is obvious for  $T$  and  $C$  in Fig. 2 but also the velocity wave is not planar (cf. later). None of the waves is pure harmonic; their shapes [shown in Fig. 2(d) at  $z = \frac{1}{2}$ ] are distorted to varying degrees. In particular, the  $C$  wave is steplike reflecting the alternating sequence of roll-like domains with high and low alcohol content: In the white (shaded) patch of Fig. 2(c) centered on and comoving with the left- (right-) turning vortex the concentration is practically constant and small (large). The boundaries of the white and shaded patches in Fig. 2(c) practically coincide with the separatrices<sup>5</sup> of the stream function in the frame comoving with the TW. The separatrices close to the upper (lower) plate where the conductive concentration profile is high (low) are rich (poor) in alcohol. The other isoconcentration lines in Fig. 2(c) also practically coincide with streamlines in the comoving frame. Thus, except for diffusion (which, however, is small with  $L$  being small) alcohol inside the separatrices is trapped there, comoving with the TW. On the other hand, alcohol outside the separatrices moves basically opposite to the TW along open streamlines that are very similar to the open isoconcentration lines in Fig. 2(c). All in all, the mixture undergoes a separation into distinct roll-like domains of alternating high and low alcohol content with a thin, meandering

boundary layer between them (by contrast, stationary rolls are mirror images of each other and  $C$  is almost constant in the middle portion of the layer). The concentration profile in the layer is linear<sup>11</sup> [cf. Fig. 2(d)]. With increasing  $\omega$  the spatial extent of the layer grows, the separatrices, i.e., the size of the patches, shrink, and the concentration contrast increases.

The TW shows symmetry behavior under translation

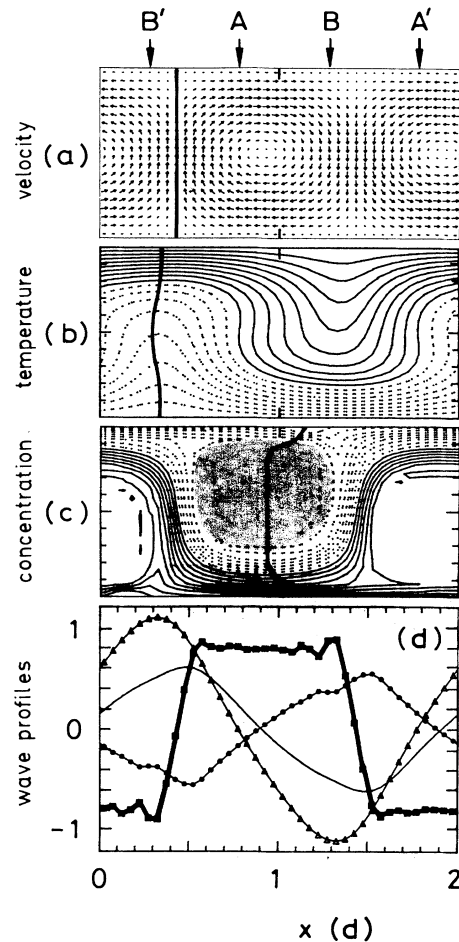


FIG. 2. TW traveling to the right: (a) velocity field; (b), (c) equidistant isolines for  $T, C$  in the  $x$ - $z$  section of the layer. Full (dotted) isolines refer to small (large) values. Crest positions (thick lines) of first lateral harmonics show that the waves are not planar and that they are phase shifted relative to each other. Wave forms (d) of  $0.04w$  (thin line),  $4\theta$  (triangles),  $10c$  (thick lines with squares), and  $2\bar{\rho}$  (dots) at  $z = \frac{1}{2}$  are not harmonic. Square-shaped concentration wave reflects the separation into right-turning rolls with high alcohol concentration and left-turning rolls with low  $C$ . Shaded (white) patch of constant large (small)  $C$  is bounded by separatrix of stream function in frame comoving with TW. Open iso- $C$ -lines practically agree with open streamlines in that frame. Parameters are  $\sigma = 10$ ,  $L = 0.01$ ,  $\psi = -0.6$ ,  $r = 1.037 r_{osc}$ ,  $\omega = 0.347 \omega_H$ ,  $\lambda = 2$ .

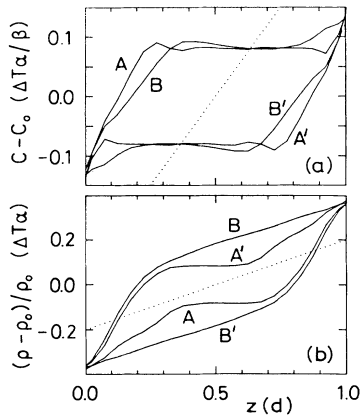


FIG. 3. Vertical field profiles at positions  $A, A'$  (near roll centers) and  $B, B'$  (near downflow and upflow, respectively) marked by arrows in Fig. 2. Dotted lines are conductive profiles. Fields at  $A, A'$  and  $B, B'$  are related to each other by the discrete symmetry operation (2).

in  $x$  by  $\lambda/2$  combined with reflection at the midplane,

$$\delta F(x, z) = \pm \delta F(x + \lambda/2, 1 - z), \quad \delta F = F - F_0, \quad (2)$$

with  $+$  for  $u, p$  and  $-$  for  $w, T, C, \rho$ . Stationary roll patterns in mixtures and in pure fluids also have this symmetry which, as far as we know, has not been mentioned in the literature.

In Fig. 3 we show vertical  $C$  and  $\rho$  profiles at positions  $A, A'$  (near roll centers) and  $B, B'$  (near downflow and upflow, respectively) marked by arrows in Fig. 2 together with linear conductive profiles (dotted lines). Convection changes the  $C$  profile drastically and almost halves the conductive concentration difference between alcohol-rich fluid at the top and alcohol-poor fluid at the bottom. However, this is not done by mixing the fluid homogeneously but by mixing it on two concentration levels of alcohol-rich rolls (positions  $A, B$ ) and alcohol-poor rolls (positions  $A', B'$ ) with boundary layers between them and the plates. The convection-induced reduction in the vertical concentration contrast enhances for  $\psi < 0$  the density contrast between top and bottom (by almost 85%), thus increases the already unstable conductive density stratification even more, and thereby increases the buoyancy force that drives convection. This nonlinear feedback mechanism might explain why the intensity of convection does not grow linearly with applied temperature stress out of the conductive state but rather shows a first-order transition in a backwards bifurcation.

To quantify the anharmonicity of the waves we show in Fig. 4 lateral Fourier amplitudes  $|f_n(z)|$  of the convective fields (1) in comparison with critical modes resulting from linear analysis<sup>10</sup> at  $r_{osc}$ . We do not show velocity modes since, e.g.,  $|u_1|$  and  $|w_1|$  are practically identical to stationary convective modes in pure water and the shape of the former agrees with the linear

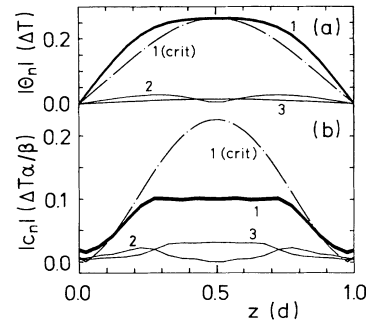


FIG. 4. Fourier amplitudes  $|f_n|$  of convective TW fields for  $n=1,2,3$  vs  $z$ . Curves labelled "crit" result from a linear analysis at  $r_{osc}$  with an overall scaling factor chosen such that  $|\theta_1|$  for linear and nonlinear TW states agree at  $z = \frac{1}{2}$ .

modes. The plateaulike behavior of  $|c_1|$  in the fully developed TW clearly differs from the critical concentration mode. Both of the latter, however, show similar small-scale boundary-layer variations near  $z=0$  and  $1$  caused by the small Lewis number. While  $n > 1$  harmonics of  $\mathbf{u}$  and  $\theta$  carry only small weight this does not hold for  $c$ .

We finally discuss the mean lateral flow  $U(z) = \langle u \rangle$  and mean lateral convective currents of heat,  $\langle Tu \rangle$ , concentration,  $\langle Cu \rangle$ , and mass,  $\langle \rho u \rangle$ . The angular bracketing implies a lateral average or equivalently a time average over one period of the TW. The mean flow results from Reynolds stresses of the TW velocity field that are related<sup>5</sup> to  $z$ -dependent phases of  $w_n(z)$ . The mean flow profile and the phase,  $\varphi_w(z)$ , of the  $n=1$  mode of  $w$  are shown in Fig. 5(a). Both are bowed opposite to  $\mathbf{k}$ . Because of (2) they are symmetric around  $z = \frac{1}{2}$ . As an aside we mention that  $\varphi_w$  in the linear TW at  $r_{osc}$  is curved towards  $\mathbf{k}$  but changes direction with decreasing

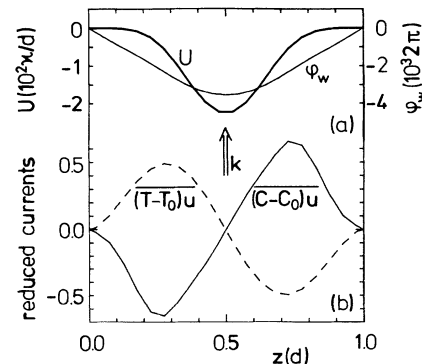


FIG. 5. (a) Lateral mean flow  $\langle u \rangle = U(z)$  and phase  $\varphi_w(z)$  of the first Fourier mode  $w_1$ . (b) Contribution (ii) to mean lateral currents of heat and of concentration. The TW propagates into the direction of the arrow. The overbar in the figure has the same meaning as the angular brackets in text.

$\sigma$ . In our nonlinear TW the direction changes near the saddle. With  $|w_1|$  varying quadratically near the plates and  $\varphi_w$  growing linearly there,  $U(z)$  grows with the fifth power of the distance from the plates. The maximal mean flow is about 1% of the phase velocity of the TW and the total spatial mean is  $U_0 = \int_0^1 dz U(z) \approx -0.008$ .

Note that the two contributions (i)  $F_0U$  and (ii)  $\langle(F - F_0)u\rangle$  [Fig. 5(b)] to the mean lateral convective  $F$  current,  $\langle Fu\rangle$ , are quite different: (i) describes transport of the mean  $F_0$  by the flow  $U$  while (ii), being practically identical to  $\langle fu\rangle$  for  $T$  and  $C$ , is dominated by the convective part  $f$ . The currents

$$\langle fu\rangle = \frac{1}{2k} \text{Im} \sum_{n=1} \frac{1}{n} f_n \partial_z w_n^*$$

in turn are dominated by  $|f_1| |\partial_z |w_1| \sin(\varphi_f - \varphi_w)$  which explains the direction and form of the currents in Fig. 5(b) in the upper and lower halves of the layer. Being driven mostly by the phase difference between the  $f$  and  $w$  waves they are present also<sup>5</sup> if  $U=0$ . With (2) the profiles (ii) are antisymmetric around the midplane so that the net current  $\int_0^1 dz \langle(F - F_0)u\rangle$  vanishes. But in the upper half of the layer there is a stationary current of heat  $\langle\theta u\rangle$  (concentration  $\langle cu\rangle$ ) parallel to  $\mathbf{k}$  ( $-\mathbf{k}$ ), and vice versa in the lower half. The size is not small, e.g.,  $\langle\theta u\rangle \approx 0.5$  is comparable to the vertical convective heat current,  $N-1$ . In addition, the currents (i) contribute depending on the particular experimental value of  $T_0$ ,  $C_0$ , and  $\rho_0$ . In our case the contribution  $F_0U_0$  to  $\langle Tu\rangle$  and  $\langle \rho u\rangle$  would be substantially larger than the maximum of  $\langle fu\rangle$ , while for the concentration current they would be comparable. Extended TW states (the role of lateral currents and mean flow in localized states is still an open problem) in annular experimental containers, being unobstructed by lateral sidewalls, are best

suitable to check our predictions.

Support by the Deutsche Forschungsgemeinschaft and by the Stiftung Volkswagenwerk is acknowledged by W.B. and M.K., respectively.

<sup>1</sup>J. K. Platten and J. C. Legros, *Convection in Liquids* (Springer-Verlag, Berlin, 1984). Since a later review does not exist we refer to the references in recent experimental (Ref. 2) and theoretical (Refs. 3-6) work.

<sup>2</sup>T. S. Sullivan and G. Ahlers, *Phys. Rev. Lett.* **61**, 78 (1988); J. Fineberg, E. Moses, and V. Steinberg, *ibid.* **61**, 838 (1988); P. Kolodner and C. M. Surko, *ibid.* **61**, 842 (1988); O. Lhost and J. K. Platten, *Phys. Rev. A* **38**, 3147 (1988).

<sup>3</sup>E. Knobloch and D. R. Moore, *Phys. Rev. A* **37**, 860 (1988); M. C. Cross and K. Kim, *ibid.* **37**, 3909 (1988).

<sup>4</sup>E. Knobloch, *Phys. Rev. A* **34**, 1538 (1986); H. R. Brand, P. S. Lomdahl, and A. C. Newell, *Physica (Amsterdam)* **23D**, 345 (1986); M. Cross, *Phys. Rev. Lett.* **57**, 2935 (1986); W. Schöpf and W. Zimmermann (unpublished).

<sup>5</sup>S. J. Linz and M. Lücke, *Phys. Rev. A* **35**, 3997 (1987); S. J. Linz, M. Lücke, H. W. Müller, and J. Niederländer, *ibid.* **38**, 5727 (1988).

<sup>6</sup>A. E. Deane, E. Knobloch, and J. Toomre, *Phys. Rev. A* **37**, 1817 (1988).

<sup>7</sup>C. W. Hirt, B. D. Nichols, and N. C. Romero, Los Alamos Scientific Laboratory Report No. LA-5652, 1975 (unpublished).

<sup>8</sup>P. Kolodner, H. Williams, and C. Moe, *J. Chem. Phys.* **80**, 6512 (1988).

<sup>9</sup>L. D. Landau and E. M. Lifshitz, *Fluid Mechanics* (Pergamon, New York, 1959).

<sup>10</sup>We have performed a linear stability analysis of the conductive state with a shooting method and found agreement with the other methods (Ref. 3).

<sup>11</sup>B. I. Shraiman, *Phys. Rev. A* **36**, 261 (1987).